Am J Transl Res 2026;18(7):5964-5973
www.ajtr.org /ISSN:1943-8141/AJTR0169233

Original Article

A novel Microtus fortis MCAO model for ischemic stroke: surgical validation and transcriptomic insights

Chengji Wang[1*], Hainan Yang[2*], Hui Ye[2], Weifang Yuan[2], Haikuo Wang[2], Xueru Huang[2], Lingjuan Wu[4], Meichen Liu[4], Jing Wang[4], Ruling Shen[1], Weikui Feng[3], Xiaoming Xin[4]

[1]Shanghai Laboratory Animal Research Center, Shanghai 201203, China; [2]Department of Critical Care Medicine, Seventh People's Hospital of Shanghai University of Traditional Chinese Medicine, Shanghai 200137, China; [3]Department of Neurology, Mian County Hospital, Hanzhong 724200, Shaanxi, China; [4]School of Pharmacy, Shanghai University of Medicine and Health Sciences, Shanghai 201318, China. [*]Equal contributors.

Received October 10, 2025; Accepted May 16, 2026; Epub July 15, 2026; Published July 30, 2026

Abstract: Objectives: Ischemic stroke (IS) is a leading cause of death and long-term disability worldwide. Rodent models, particularly mice and rats, are widely used to investigate its underlying mechanisms. The *Microtus fortis* (reed vole) represents a promising alternative animal model due to its anatomical similarity to mice and cost-effectiveness; however, a middle cerebral artery occlusion (MCAO) model in this species has not yet been well characterized. Methods: We established an MCAO model in *Microtus fortis*. Triphenyltetrazolium chloride (TTC) staining, neurological deficit scoring, and cerebral blood flow (CBF) measurements were used to evaluate model establishment. In addition, transcriptomic sequencing was performed on brain tissue from *Microtus fortis* following cerebral ischemia-reperfusion injury. Gene expression patterns were analyzed using correlation-based classification and functional enrichment analyses. Differentially expressed genes (DEGs) were further validated by quantitative PCR (qPCR). Results: The model demonstrated a significant reduction in CBF (58.86%, $P < 0.001$) and clear neurological deficits. A total of 1,707 DEGs were identified, including 1,379 upregulated and 328 downregulated genes, which were primarily enriched in immune and inflammatory pathways. Key genes (CCL4, LIF, IL6, and OSM [upregulated]; LOC126493158 and LOC126489791 [downregulated]) were successfully validated. Conclusion: *Microtus fortis* represents a feasible MCAO model, offering both surgical practicality and cost advantages over traditional rodent models. This study provides foundational genomic and functional insights, supporting its potential application in translational stroke research.

Keywords: Ischemic stroke, *Microtus fortis*, MCAO model, gene expression profile, translational medicine

Introduction

Stroke is now the second leading cause of both death and disability globally. Among these, ischemic stroke (IS) caused by arterial occlusion is the most common form. IS occurs due to the narrowing or blockage of arteries that supply blood to the brain, such as the carotid and vertebral arteries, resulting in inadequate blood and oxygen delivery to the brain [1, 2]. If patients fail to receive timely and effective treatment after the onset of stroke symptoms, they are at high risk of developing brain damage, which can lead to impairments in movement, speech, language, or even result in death [3, 4].

Because animal models can mimic changes in the human, they are crucial in medical research. These models are essential for studying disease mechanisms, and they are becoming increasingly diverse. Today, animal models are not only used to investigate the physiological processes involved in disease onset and progression, but also for drug target screening and gene therapy exploration [5]. Mouse models are frequently employed in stroke studies because of their genetic accessibility and relatively low cost. Among them, the middle cerebral artery occlusion (MCAO) model is considered one of the most established and widely adopted methods for simulating human IS [6-8].

During the domestication of *Microtus fortis* for experimental purposes, we observed that their brain anatomy closely resembles that of mice, indicating their potential as an alternative animal model for translational research in vascular

https://doi.org/10.62347/DFKC2591

occlusive diseases. *Microtus fortis*, commonly known as the reed vole, belongs to the family Cricetidae within the order Rodentia, and is distributed across China, Russia, North Korea, and Mongolia [9]. In recent years, *Microtus fortis* has been used in medical research on diseases such as schistosomiasis [10, 11], and ovarian cancer [12], establishing it as a promising new experimental model for studying human diseases and developmental processes. However, an MCAO model in *Microtus fortis* has not yet been clearly described.

This study will discuss design, and validate the use of *Microtus fortis* as an animal model for MCAO research. Using the NovaSeq X Plus and DNBSEQ-T7 sequencing platforms, we conducted transcriptome sequencing on both MCAO-affected and healthy brain tissues of *Microtus fortis*. This study produced a comprehensive genomic map and detailed gene function annotations, allowing for an in-depth analysis of molecular events at both the gene and transcriptional levels during the MCAO process.

Materials and methods

Animals

Female *Microtus fortis*, aged 8 weeks and weighing between 20 and 30 grams, were obtained from the Shanghai Laboratory Animal Research Center (license no. 202105902). The animals were placed in an environment with regulated parameters, where the temperature varied between 24°C and 26°C, and the relative humidity was controlled to remain within the range of 50% to 60%. A total of 11 female *Microtus fortis* (8 weeks old, 20-30 g) were used in this study. Among them, 10 animals underwent MCAO surgery, and 1 sham-operated animal served as control. The specific usage of animals for each experiment is as follows: MCAO modeling and CBF measurement: All 10 MCAO-operated animals were used for cerebral blood flow (CBF) monitoring during surgery to confirm successful occlusion. Behavioral testing: Neurological deficit scores were assessed in all 10 MCAO-operated animals at 24 h post-surgery. TTC staining: Six MCAO animals were used for infarct volume assessment via TTC staining. RNA-seq and qPCR: The remaining 4 MCAO animals (different from the 6 used for TTC staining) were used for both RNA-seq and qPCR. In these animals, brain tissues from the ischemic side and the contralateral side were collected separately. The same animals were used for both RNA-seq and qPCR, ensuring consistency between transcriptomic and validation analyses. After the experiment, the animals were given an intravenous injection of pentobarbital sodium for euthanasia. Additionally, the *Microtus fortis* in the experiment were euthanized using 240 mg/kg pentobarbital sodium for anesthesia.

MCAO model

Transient or permanent focal cerebral ischemia was induced using the intraluminal filament method. Animals were anesthetized via intramuscular injection of Zoletil 50 (40 mg/kg). Following a midline cervical incision, the left common carotid artery (CCA), external carotid artery (ECA), and internal carotid artery (ICA) were carefully exposed and isolated. The CCA and ECA were ligated with 6-0 silk sutures, and a microvascular clip was temporarily applied to the ICA. A small arteriotomy was made on the CCA between the ligation site and the ICA bifurcation. A silicone-coated monofilament (diameter: 0.22 mm; silicone tip length: 5 mm; Beijing Sunbio Biotech, China) was introduced into the CCA and advanced gently into the ICA until slight resistance was encountered. The insertion depth, approximately 1.5 cm from the CCA bifurcation, was pre-marked on the filament. Successful occlusion was verified by a $\geq$ 70% reduction in regional cerebral blood flow (rCBF), as measured by laser Doppler flowmetry (PeriFlux 5000, Sweden). The filament was maintained in position to achieve permanent occlusion. After the procedure, the incision was sutured, and the animals were allowed to recover with ad libitum access to food and water. This method constructs a permanent cerebral ischemia model. After 24 h of ischemia, the following models were used to evaluate the experiment.

Microtus fortis neurological deficit score

Neurofunctional deficits in the MCAO model were evaluated using the Longa five-point scoring system, with scores ranging from 0 to 4, where 0 indicates no impairment and 4 represents severe impairment. The scoring criteria are shown in **Table 1** [13].

Table 1. The scoring criteria of neurological deficit scores

Score	Behavior
0	No neurological deficits
1	Incomplete extension of the forelimb on the paralyzed side, indicating mild deficits
2	Circling toward the paralyzed side while walking, indicating moderate deficits
3	Falling or leaning toward the paralyzed side while walking, indicating severe deficits
4	No spontaneous walking and loss of consciousness

Cerebral blood flow measurement

Following the initial neurological assessment, the *Microtus fortis* were anesthetized and secured, and their skulls were exposed to evaluate cerebral blood flow on both the ischemic and control sides using a laser speckle contrast imaging (LSCI) system. The raw images were processed using computer algorithms and converted into blood flow velocity maps [14].

TTC staining of brain sections

The *Microtus fortis* were sacrificed, and their brain tissues were quickly removed and placed in a -20°C freezer for 20 minutes. The brains were then sliced into six coronal sections, each 2 mm thick. These slices were immersed in 2.0% 2,3,5-triphenyltetrazolium chloride (TTC) solution and incubated in the dark at 37°C for 30 minutes. The stained slices were then photographed, and image analysis software was employed to calculate infarct volume and assess brain edema [15].

RNA extraction and sequencing

Total RNA was extracted from both the experimental and control groups using Trizol reagent. The concentration and purity of the isolated RNA were assessed using a spectrophotometer, while agarose gel electrophoresis was employed to evaluate RNA integrity. The RNA quality number (RQN) was determined using an Agilent 5300. Subsequently, mRNA was isolated from total RNA through A-T base pairing with oligo(dT)-coated magnetic beads, followed by fragmentation into small segments approximately 300 bp in length. First- and second-strand cDNA synthesis was performed on individual mRNA molecules. The ends of the cDNA fragments were then converted from sticky to blunt ends using an End Repair Mix, followed by the addition of a single nucleotide adenosine (A) to the 3' end. Finally, the products were purified and size-selected after ligating adapters, and these selected products were subjected to PCR amplification to construct a library. High-throughput sequencing was planned using the NovaSeq X Plus and DNBSEQ-T7 platforms.

Bioinformatics analysis

To obtain high-quality data for downstream analysis, sequencing platforms first convert image signals into raw textual data, followed by statistical methods for quality control (QC) of the sequences. After QC, the data are aligned to a reference genome, enabling subsequent analyses such as differential gene expression, clustering, Gene Ontology (GO) analysis, and Kyoto Encyclopedia of Genes and Genomes (KEGG) pathway analysis. Genes with a $P < 0.05$ and fold change > 2 were considered significantly differentially expressed (DEGs).

Quantitative polymerase chain reaction (qPCR)

Total RNA was extracted from the brain tissue of mice using TRIzol reagent. For cDNA synthesis, 1,000 ng of RNA was reverse-transcribed with the first-strand synthesis kit for PCR, following the manufacturer's guidelines. The cDNA was used as a template in qPCR to analyze the mRNA expression levels of C-C motif chemokine ligand 4 (CCL4), leukemia inhibitory factor (LIF), interleukin 6 (IL6), ankyrin repeat domain 2 (ANKRD2), coagulation factor II thrombin receptor like 1 (F2RL1), interleukin 1 receptor type 2 (IL1R2), macrophage scavenger receptor 1 (MSR1), oxidized low-density lipoprotein receptor 1 (OLR1), LOC126493158, and LOC126489791 along with selected DEGs. **Table 2** provides a list of all primer sequences employed in this study, along with their corresponding accession numbers. The relative expression was calculated using the $2^{-\Delta\Delta Ct}$ method [16].

Table 2. Primer sequences

Gene name	Gene ID	Forward primer sequences (5'→3')	Reverse primer sequences (5'→3')
interleukin-6 family cytokine (LIF)	126500979	atcgcaggtggtactcagacatgg	gtttccagtgcagaaccagcag
triggering receptor expressed on myeloid cells 1 (TREM1)	126494960	gctgtgttgtcggccagg	gcatggcactgcctctgaca
macrophage scavenger receptor 1 (MSR1)	126504787	cactgcggtcttcttttccagc	aggaagcaatgttgtcattgagcga
interleukin 6 (IL6)	126491159	cctcagggaagtcttcgaaatgaga	agtccagaaatgggcttggatca
interleukin-1 receptor type 2 (IL1R2)	126496982	tttctggaacccctactacgcc	tttgcgagtaggagacaaatggc
F2R like trypsin receptor 1 (F2RL1)	126508583	tctcctgcaaccggacctt	tcaatggaaaagccgggttctact
oxidized low density lipoprotein receptor 1 (OLR1)	126493243	aacttctgcaacagaacgtgaacc	ctgagcatccaaagacaggcaa
ankyrin repeat domain 2 (ANKRD2)	126505000	gttccgcagatacctgcgatg	gctcccaagctccctgg
C-C motif chemokine ligand 4 (CCL4)	126495784	gcactccagcgctctcag	agctggtttggagcagaggc
LOC126493158	126493158	gaagtgagagtgccctctgtg	gaagtgagagtgccctctgtg
LOC126489791	126489791	cagaatcaagcgattcctggctaa	cccagcttcgttctcctcca

Statistical analysis

All experiments were performed with at least three biological replicates, and data are presented as mean ± SD. Differential expression analysis was conducted using edgeR. *P* values were adjusted for multiple testing using the Benjamini-Hochberg false discovery rate (FDR) method. Statistical analyses were performed using GraphPad Prism 8. Normality and homogeneity of variance were assessed prior to analysis, and $P < 0.05$ was considered statistically significant.

Results

Successful establishment of MCAO model in Microtus fortis

As shown in **Figure 1A**, TTC staining of brain tissue sections revealed ischemia-induced neuropathological damage, clearly differentiating infarcted regions from normal brain areas. In the model group, infarcted areas appeared white, whereas in the control group, brain sections consistently exhibited a uniform red color, indicating the absence of infarction. These results validate the successful establishment of the MCAO model in *Microtus fortis*. To evaluate the impact of brain ischemia on neurological function, the Longa score was used to assess behavioral changes across groups (**Figure 1B**). Compared with the control group, the MCAO group displayed significantly higher Longa scores ($P < 0.001$), indicating that reperfusion injury following brain ischemia markedly contributes to behavioral deficits. LSCI was employed to assess cerebral blood flow (CBF). As shown in **Figure 1C**, **1D**, LSCI performed 24 hours after ischemia revealed normal CBF in the control group. In contrast, the MCAO group exhibited a marked reduction in CBF on the surgical side compared with the contralateral hemisphere. Quantitative analysis showed no significant differences in CBF within the control group, whereas CBF in the ischemic hemisphere of the MCAO group was approximately 58.86% lower than that of the contralateral side.

Transcriptomic profiling identifies key DEGs in MCAO

Principal component analysis (PCA) demonstrated clear separation between the MCAO and control groups at the transcriptomic level (**Figure 2A**). Gene expression profiles showed high overlap and consistency between samples (**Figure 2B**). Bioinformatics analysis identified 1,707 differentially expressed genes (DEGs) in the brains of MCAO *Microtus fortis*, visualized by a volcano plot (**Figure 2C**).

In the plot, the x-axis represents the log-transformed ratio of expression levels between the model group and the control group. This transformation creates a symmetrical distribution of upregulated and downregulated genes. The y-axis shows the statistical significance (*p*-value) of expression differences. Gray dots represent non-significant DEGs. Genes with more significant expression differences are located closer to the edges and the top of the plot. Compared to the control group, 1,707 genes exhibited differential expression in the MCAO group. Among them, 1,379 genes (red dots) were significantly upregulated, while 328 genes (blue dots) were significantly downregulated.

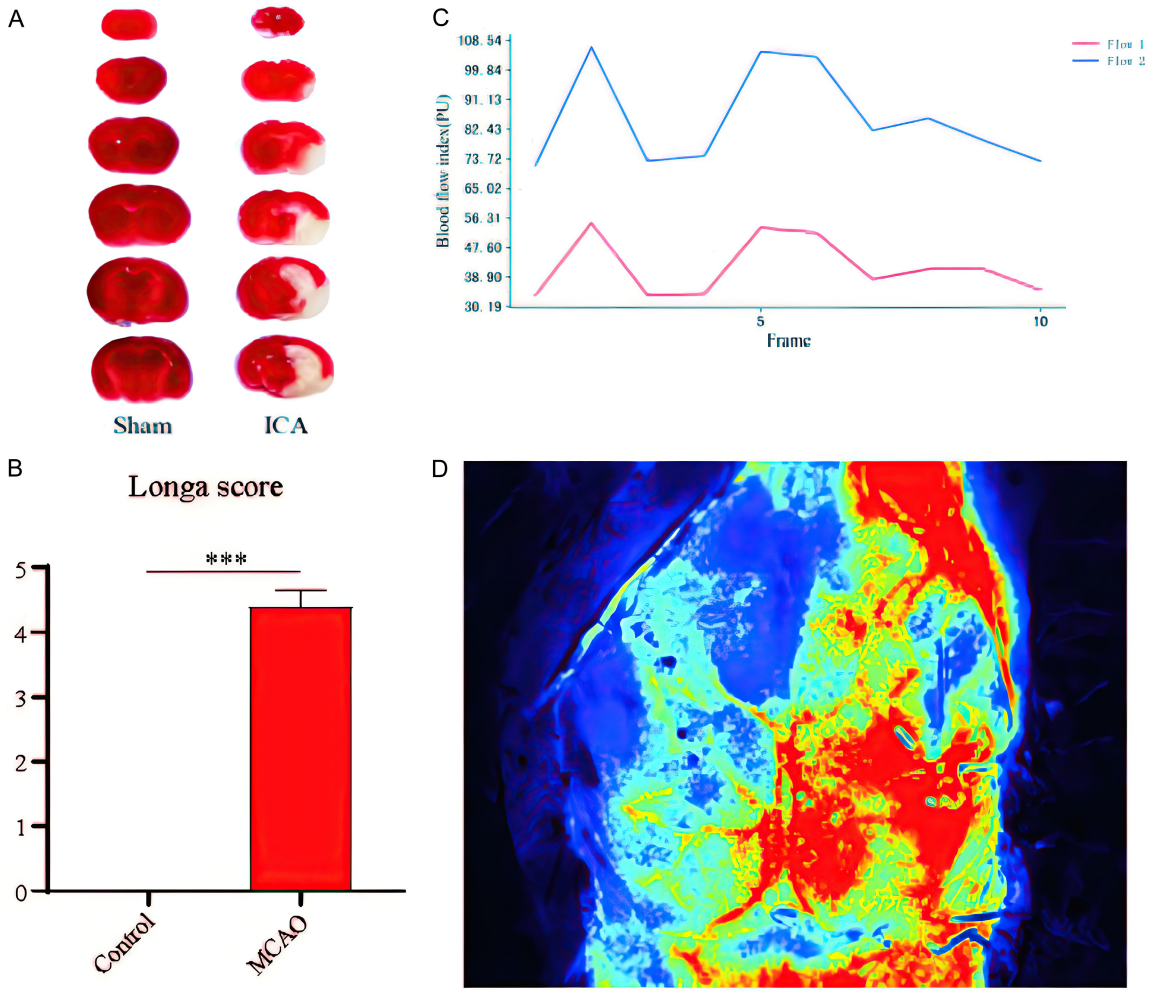

Figure 1. A. Brain slices were stained with 2,3,5-triphenyltetrazolium chloride (TTC) 24 hours following middle cerebral artery occlusion (MCAO). White regions indicate ischemic areas, while red regions represent normal tissue. B. Bar graph showing Longa scores for the MCAO groups and control groups. C. Line graph illustrating cerebral blood flow (CBF) and relative CBF in the ischemic hemisphere during surgery (n = 3). D. Representative laser speckle images depicting CBF following MCAO, ***$P < 0.001$.

These 351 DEGs may play a role in the pathological processes of MCAO, and their functional an-notations may offer valuable insights into the molecular mechanisms associated with MCAO. The heatmap shows the top 10 of up-regulated and down-regulated genes (**Figure 2D**). The up-regulated genes are CCL4, LIF, IL6 and OSM. They are involved in responses to various stimuli, inflammatory responses, and cell signaling.

Functional enrichment implicates immune and inflammatory pathways

Gene Ontology (GO) analysis was conducted to explore the functional roles of DEGs [17]. As shown in **Figure 3A**, the DEGs were classified into three functional categories: molecular function (MF), cellular component, and biological process (BP). Within the BP category, the top three enriched terms were immune system process, positive regulation of immune system process, and immune response. In the MF category, the main enriched terms were signaling receptor binding and immune receptor activity. Key genes in these categories, including CCL4, LIF, IL6, and OSM, are involved in stimulus response, inflammatory regulation, and cell signaling. These findings suggest that MCAO triggers alterations in biological processes, molecular functions, and cellular components.

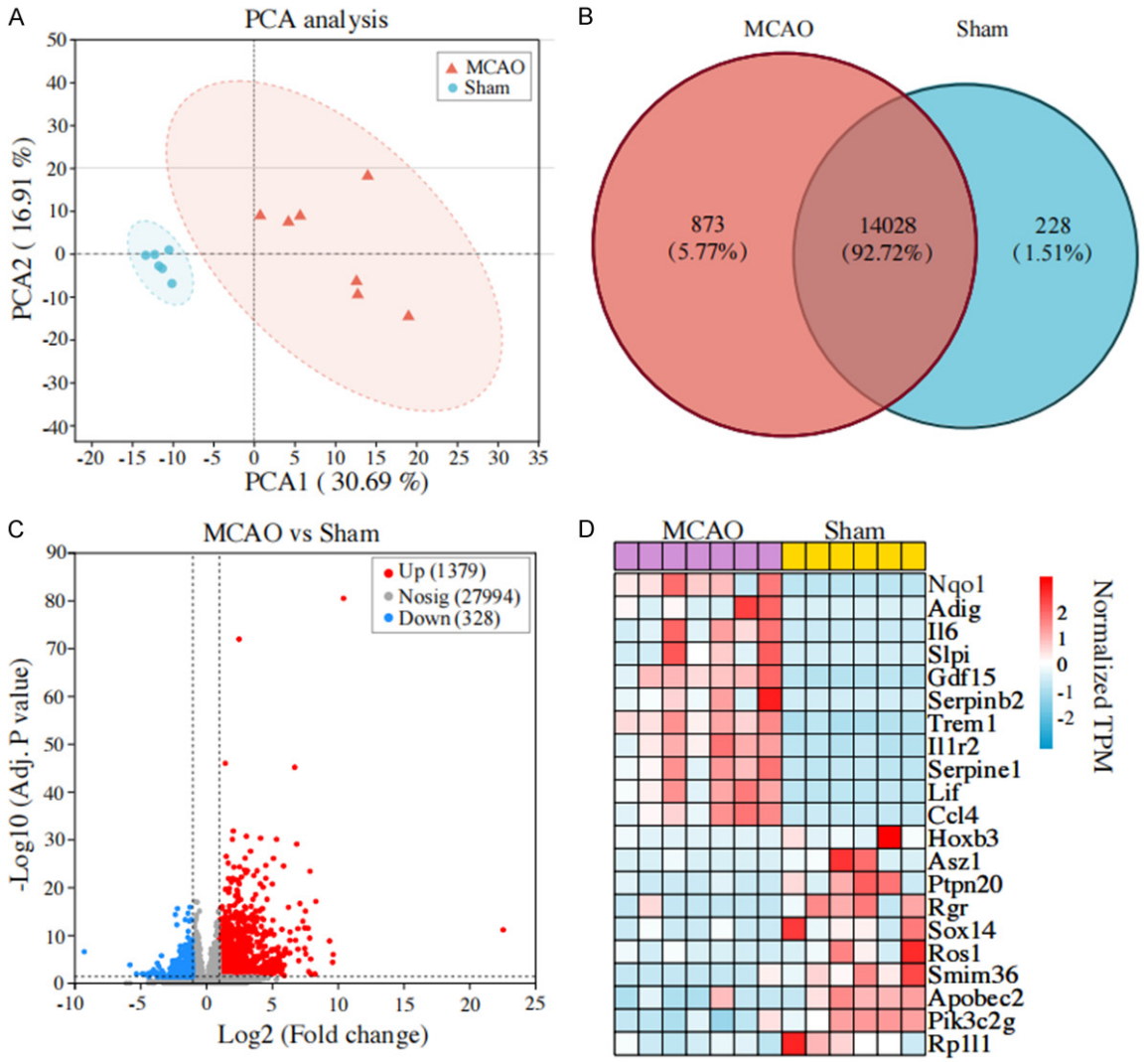

Figure 2. (A) Principal component analysis (PCA) distinguishes the MCAO group from the control group. (B) Venn diagram showing 14,028 genes that are co-expressed in the Sham group and the MCAO group. In (B), 14,028 denotes the total number of expressed genes detected in both the Sham and MCAO groups. (C) Volcano plot comparing the transcriptomes of MCAO versus Sham groups. In (C), the volcano plot illustrates the 1,707 Differentially expressed genes (DEGs) identified from these genes using the criteria $|\log_2(\text{fold change})| \geq 1$ and adjusted $P < 0.05$. (D) Heatmap displaying the top 10 upregulated and downregulated genes.

Pathway enrichment analysis of DEGs was further conducted to explore their functional implications and potential interactions [18, 19]. Using the KEGG database, DEGs were mapped to 45 pathway subclasses spanning seven major categories: Metabolism, Genetic Information Processing, Environmental Information Processing, Cellular Processes, Organismal Systems, and Human Diseases. The top three enriched pathways were osteoclast differentiation, cytokine-cytokine receptor interaction, and cell adhesion molecules. Overall, functional enrichment analysis indicated that most upregulated DEGs were associated with immune and inflammatory responses, whereas downregulated DEGs were primarily linked to the ubiquitin-proteasome system and oxidative phosphorylation (**Figure 3B**).

qPCR validation of DEGs

Verification of DEGs. CCL4, LIF, IL6, OSM, ANKRD2, F2RL1, IL1R2, MSR1, OLR1, and TREM1 were overexpressed in the MCAO group (**Figure 4**). They usually play a crucial role in mediating immune responses and during the

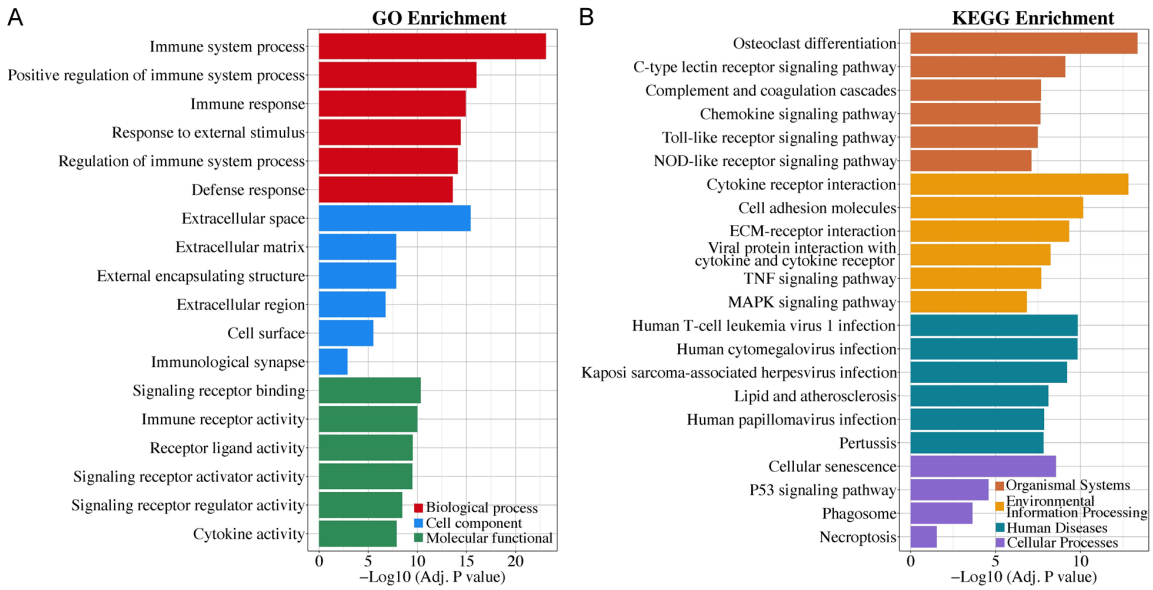

Figure 3. A. Gene Ontology (GO) functional classification of DEGs between control and MCAO groups. B. Kyoto Encyclopedia of Genes and Genomes (KEGG) pathway enrichment analysis of DEGs.

inflammatory process. LOC126493158 and LOC126489791 showed lower expression in the MCAO group in both RNA-seq and qRT-PCR analyses. The consistent results between RNA-seq and qRT-PCR validated the reliability of the RNA-seq data.

Discussion

Animal models are indispensable tools to simulate the stroke process, which can be utilized to investigate stroke pathogenesis and develop new treatment options. As a heterogeneous disease with complex pathophysiology, it is impossible to imitate all aspects of human stroke using one animal model. Each model has unique advantages and disadvantages [20, 21]. *Microtus fortis*, although geographically restricted and not widely used in biomedical research, has garnered increasing scientific research interest since its designation as a Chinese laboratory animal resource in 2021 [22]. However, research progress remains hindered by the limited understanding of its genomic resources. This study established an MCAO model in the *Microtus fortis* and explored the molecular characteristics of cerebral ischemia-reperfusion in this species through RNA sequencing and bioinformatics analysis.

Changes in gene expression following cerebral ischemia provide critical insights into the molecular and cellular mechanisms underlying stroke, which may be important for advancing clinical treatment. This study used CBF monitoring to assess whether internal carotid artery embolism blocked blood flow to the left hemisphere. The results indicated a significant decrease of approximately 58.86%. Pathological evaluation of post-reperfusion ischemic injury was further performed using TTC staining, in which brain sections from the MCAO group showed clearly visible white regions on gross examination, indicating ischemic damage. Moreover, motor dysfunction caused by cerebral ischemia was assessed using neurological behavioral scoring. We employed Illumina sequencing technology to examine RNA transcriptomic changes in *Microtus fortis* before and after cerebral ischemia. Additionally, we conducted an integrated analysis of nine publicly available GEO datasets to identify stroke-related mechanisms and biological functions.

Chemotaxis was notably enriched among biological processes, with up-regulated genes significantly associated with chemokine-cytokine receptor interactions and chemokine signaling pathways, including TNF and NF-κB signaling pathways, as well as cytokine-cytokine receptor interactions. These findings align with previous RNA sequencing studies in rats and mice underscoring the importance of inflammation

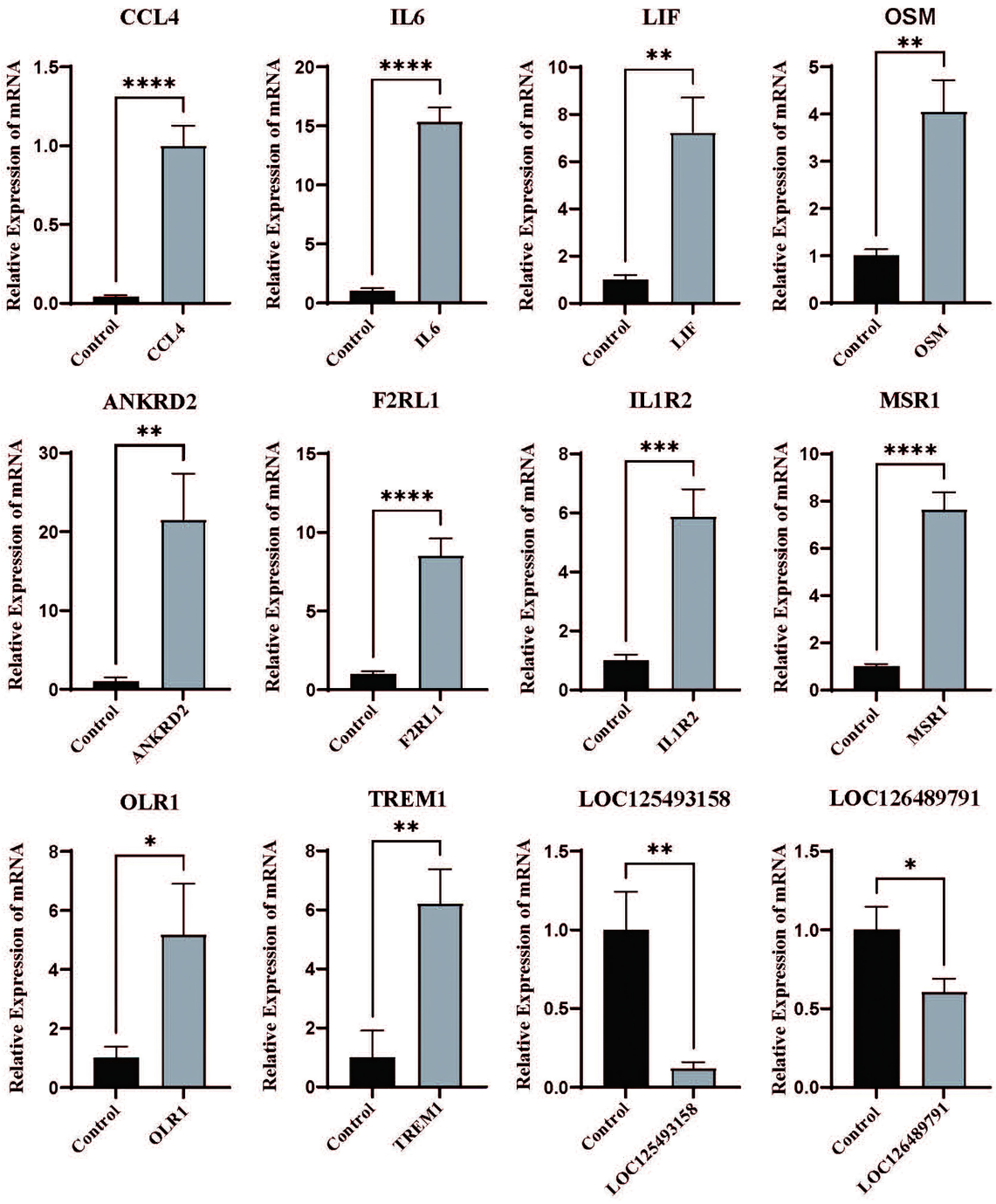

Figure 4. Bar plot showing quantitative polymerase chain reaction (qPCR) validation of DEG expression. *P < 0.05, **P < 0.01, ***P < 0.001, ****P < 0.0001.

in IS [23, 24]. During stroke, the activation of astrocytes and microglia is rapidly enhanced, promoting the production of pro-inflammatory cytokines (e.g., IL-1β, IL-6, and TNF) through pathways such as MAPK signaling. This leads to the infiltration of focal neutrophils and peripheral lymphocytes, exacerbating central nervous system injury [25]. Among these factors, TNF and IL-6 have been the most extensively studied in cerebral ischemia [26]. Furthermore, we validated the RNA-Seq results by performing qPCR analysis on four up-regulated DEGs (CCL4, LIF, IL6, OSM) and two down-regulated DEGs (LOC126493158, LOC126489791) relat-

ed to inflammation, immune response, and stress response [27].

Conclusions and perspectives

This study has several limitations. First, although both male and female animals were included, the sample size was insufficient to permit a robust sex-based subgroup analysis; therefore, potential sex-related differences in outcomes could not be assessed. Future studies with larger cohorts are warranted to address this issue. In addition, the experimental design did not include longitudinal observations to monitor disease progression, nor did it incorporate comparisons with commonly used laboratory rodent models. Nevertheless, the biological structure and functional characteristics of *Microtus fortis* suggest that it represents a promising novel animal model for IS. Its use may offer an additional resource for translational medical research. Compared with more widely used experimental species such as mice and rats, *Microtus fortis* presents distinct advantages: it is larger than mice, which facilitates surgical procedures, yet smaller than rats, thereby reducing compound consumption in pharmacological studies and lowering overall experimental costs. In summary, *Microtus fortis* shows considerable potential to be developed as a new experimental animal resource.

Acknowledgements

This work was supported by the National Key Research and Development Program of China (Grant No. 2021YFF0702403), the Scientific Research Program of Shanghai Pudong New Area Health Commission (Grant No. PW2024A-58), and the Discipline Construction Plan of Pudong New Area Health Commission (Grant No. PWZxq2022-09).

Disclosure of conflict of interest

None.

Address correspondence to: Dr. Ruling Shen, Shanghai Laboratory Animal Research Center, Shanghai 201203, China. Tel: +86-0215-0793648; E-mail: shenruling@slarc.org.cn; Dr. Weikui Feng, Department of Neurology, Mian County Hospital, Lüyuan Road, Dingjunshan Town, Mian County, Hanzhong 724200, Shaanxi, China. Tel: +86-0916-3232005; E-mail: fengweikui@126.com; Dr. Xiaoming Xin, School of Pharmacy, Shanghai University of Medicine and Health Sciences, Shanghai 201318, China. Tel: +86-0216-5881635; E-mail: xinxm@sumsh.edu.cn

References

[1] Ji P, Xu Q, Li J, Wang Z, Mao W and Yan P. Advances in nanoparticle-based therapeutics for ischemic stroke: enhancing drug delivery and efficacy. Biomed Pharmacother 2024; 180: 117564.

[2] Peng B, Mohammed FS, Tang X, Liu J, Sheth KN and Zhou J. Nanotechnology approaches to drug delivery for the treatment of ischemic stroke. Bioact Mater 2025; 43: 145-161.

[3] Barthels D and Das H. Current advances in ischemic stroke research and therapies. Biochim Biophys Acta Mol Basis Dis 2020; 1866: 165260.

[4] Rathore SS, Hinn AR, Cooper LS, Tyroler HA and Rosamond WD. Characterization of incident stroke signs and symptoms: findings from the atherosclerosis risk in communities study. Stroke 2002; 33: 2718-2721.

[5] Li Z, Zheng W, Wang H, Cheng Y, Fang Y, Wu F, Sun G, Sun G, Lv C and Hui B. Application of animal models in cancer research: recent progress and future prospects. Cancer Manag Res 2021; 13: 2455-2475.

[6] Fluri F, Schuhmann MK and Kleinschnitz C. Animal models of ischemic stroke and their application in clinical research. Drug Des Devel Ther 2015; 9: 3445-3454.

[7] Sokolowski JD, Soldozy S, Sharifi KA, Norat P, Kearns KN, Liu L, Williams AM, Yağmurlu K, Mastorakos P, Miller GW, Kalani MYS, Park MS, Kellogg RT and Tvrdik P. Preclinical models of middle cerebral artery occlusion: new imaging approaches to a classic technique. Front Neurol 2023; 14: 1170675.

[8] Zeng L, Hu S, Zeng L, Chen R, Li H, Yu J and Yang H. Animal models of ischemic stroke with different forms of middle cerebral artery occlusion. Brain Sci 2023; 13: 1007.

[9] Shen J, Xiang S, Peng M, Zhou Z and Wu Z. Mechanisms of resistance to *Schistosoma japonicum* infection in *Microtus fortis*, the natural non-permissive host. Front Microbiol 2020; 11: 2092.

[10] Dibo N, Zhou Z, Liu X, Li Z, Zhong S, Liu Y, Duan J, Xia M, Ma Z, Wu X and Huang S. Time-course whole blood transcriptome profiling provides new insights into *Microtus fortis* natural resistance mechanism to *Schistosoma japonicum*. Heliyon 2024; 10: e38067.

[11] Zhang D, Hu Q, Liu X, Liu X, Gao F, Liang Y, Zou K, Su Z, Zhi W and Zhou Z. A longitudinal study

reveals the alterations of the *Microtus fortis* colonic microbiota during the natural resistance to Schistosoma japonicum infection. Exp Parasitol 2020; 219: 108030.

[12] Hu Q, Gao M, Zhang D, Leng B, Wang J, Liu Q, He S, Zhi W and Zhou Z. *De novo* assembly and transcriptome characterization: novel insights into the mechanisms of primary ovarian cancer in *Microtus fortis*. Mol Med Rep 2022; 25: 64.

[13] Guo K and Lu Y. Acupuncture modulates the AMPK/PGC-1 signaling pathway to facilitate mitochondrial biogenesis and neural recovery in ischemic stroke rats. Front Mol Neurosci 2024; 17: 1388759.

[14] Wang J, Li Y, Yu H, Li G, Bai S, Chen S, Zhang P and Tang Z. Dl-3-N-butylphthalide promotes angiogenesis in an optimized model of transient ischemic attack in C57BL/6 mice. Front Pharmacol 2021; 12: 751397.

[15] Guo Y, Mao M, Li Q, Yu X and Zhou L. Extracts of Ginkgo flavonoids and ginkgolides improve cerebral ischaemia-reperfusion injury through the PI3K/Akt/Nrf2 signalling pathway and multicomponent in vivo processes. Phytomedicine 2022; 99: 154028.

[16] Cheng X, Yang YL, Li WH, Liu M, Wang YH and Du GH. Cerebral ischemia-reperfusion aggravated cerebral infarction injury and possible differential genes identified by RNA-Seq in rats. Brain Res Bull 2020; 156: 33-42.

[17] Huang da W, Sherman BT and Lempicki RA. Bioinformatics enrichment tools: paths toward the comprehensive functional analysis of large gene lists. Nucleic Acids Res 2009; 37: 1-13.

[18] Franceschini A, Szklarczyk D, Frankild S, Kuhn M, Simonovic M, Roth A, Lin J, Minguez P, Bork P, von Mering C and Jensen LJ. STRING v9.1: protein-protein interaction networks, with increased coverage and integration. Nucleic Acids Res 2013; 41: D808-815.

[19] Ashburner M, Ball CA, Blake JA, Botstein D, Butler H, Cherry JM, Davis AP, Dolinski K, Dwight SS, Eppig JT, Harris MA, Hill DP, Issel-Tarver L, Kasarskis A, Lewis S, Matese JC, Richardson JE, Ringwald M, Rubin GM and Sherlock G. Gene ontology: tool for the unification of biology. The Gene Ontology Consortium. Nat Genet 2000; 25: 25-29.

[20] Li Y and Zhang J. Animal models of stroke. Animal Model Exp Med 2021; 4: 204-219.

[21] Bogousslavsky J, Van Melle G and Regli F. The Lausanne Stroke Registry: analysis of 1,000 consecutive patients with first stroke. Stroke 1988; 19: 1083-1092.

[22] Li YS, Zheng MM, Jiang BY, Tu HY, Yang JJ, Zhang XC and Wu YL. Association of cerebrospinal fluid tumor DNA genotyping with survival among patients with lung adenocarcinoma and central nervous system metastases. JAMA Netw Open 2020; 3: e209077.

[23] Duan X, Gan J, Xu F, Li L, Han L, Peng C, Bao Q, Xiao L and Peng D. RNA sequencing for gene expression profiles in a rat model of middle cerebral artery occlusion. Biomed Res Int 2018; 2018: 2465481.

[24] Li L, Dong L, Xiao Z, He W, Zhao J, Pan H, Chu B, Cheng J and Wang H. Integrated analysis of the proteome and transcriptome in a MCAO mouse model revealed the molecular landscape during stroke progression. J Adv Res 2020; 24: 13-27.

[25] Zhou H, Qiu Z, Gao S, Chen Q, Li S, Tan W, Liu X and Wang Z. Integrated analysis of expression profile based on differentially expressed genes in middle cerebral artery occlusion animal models. Int J Mol Sci 2016; 17: 776.

[26] Han HS and Yenari MA. Cellular targets of brain inflammation in stroke. Curr Opin Investig Drugs 2003; 4: 522-529.

[27] Filippenkov IB, Remizova JA, Denisova AE, Stavchansky VV, Golovina KD, Gubsky LV, Limborska SA and Dergunova LV. Differential gene expression in the contralateral hemisphere of the rat brain after focal ischemia. Sci Rep 2023; 13: 573.